Ultrafast Atomic Diffusion Inducing a Reversible $(2\sqrt{3}\times 2\sqrt{3})R30° \leftrightarrow (\sqrt{3}\times\sqrt{3})R30°$ Transition on Sn/Si(111):B

W. Srour,[1,2] Daniel G. Trabada,[3] J. I. Martínez,[3] F. Flores,[3] J. Ortega,[3] M. Abuín,[4] Y. Fagot-Revurat,[1] B. Kierren,[1] A. Taleb-Ibrahimi,[5] D. Malterre,[1] and A. Tejeda[2,6,*]

[1]*Institut Jean Lamour, CNRS-Université de Lorraine, 54506 Vandoeuvre les Nancy, France*
[2]*Synchrotron SOLEIL, L'Orme des Merisiers, Saint-Aubin, 91192 Gif sur Yvette, France*
[3]*Dto. de Física Teórica de la Materia Condensada and Condensed Matter Physics Center (IFIMAC), Universidad Autónoma de Madrid, 28049 Madrid, Spain*
[4]*Dto. de Física de Materiales, Universidad Complutense de Madrid, 28040 Madrid, Spain*
[5]*UR1 CNRS/Synchrotron SOLEIL, Saint-Aubin, 91192 Gif sur Yvette, France*
[6]*Laboratoire de Physique des Solides, Université Paris-Sud, CNRS, UMR 8502, F-91405 Orsay, France*

(Received 5 September 2014; published 13 May 2015)

Dynamical phase transitions are a challenge to identify experimentally and describe theoretically. Here, we study a new reconstruction of Sn on silicon and observe a reversible transition where the surface unit cell divides its area by a factor of 4 at 250 °C. This phase transition is explained by the 24-fold degeneracy of the ground state and a novel diffusive mechanism, where four Sn atoms arranged in a snakelike cluster wiggle at the surface exploring collectively the different quantum mechanical ground states.

DOI: 10.1103/PhysRevLett.114.196101 PACS numbers: 68.35.Ja, 68.35.Rh, 68.37.Ef, 68.43.Bc

Metallic overlayers on semiconductor surfaces are prone to phase transitions [1–3], and many exotic phenomena have been found in these two dimensional systems, such as low-dimensional superconductivity [4,5], magnetic orderings [6,7], and metal-insulator transitions [8–17]. In temperature-induced transitions, very often the dynamical fluctuation of surface atoms is associated with changes of the structural and/or electronic properties of the system. Two paradigms of dynamical fluctuations are In/Si(111) [18–20] and Sn/Ge(111) [21–25]. In Sn/Ge(111), a first transition appears around 200 K, the system changing its symmetry from $(\sqrt{3}\times\sqrt{3})R30°$ to (3×3) as observed by low energy electron diffraction (LEED) and scanning tunneling microscopy (STM) [21]. This transition was explained in terms of the dynamical fluctuations of the system between the threefold degenerate ground states associated with the (3×3)-structure [23]. At high temperature, the system presents on average a $(\sqrt{3}\times\sqrt{3})R30°$ as seen with slow probes (LEED and STM) but, locally, it keeps a (3×3) structure as observed with fast probes (core level spectroscopy). In In/Si(111), there is a reversible $(4\times1) \leftrightarrow (8\times2)$ phase transition that is accompanied by a metal-insulator one [18]. The (4×1) reconstruction consists of two zigzag rows of In atoms forming quasione dimensional chains, separated by zigzag rows of Si atoms. The (8×2) phase is formed by weakly coupled chains each one with a (4×2) reconstruction. At low temperature, each (4×2) chain is frozen in one of its four degenerate states while, at high temperature, molecular dynamics (MD) simulations show that the chain fluctuates between its different ground states presenting on average a (4×1) symmetry [19]. These fluctuations of the In zigzag rows are responsible for the metallicity of the system at high temperature.

Here, we present experimental and theoretical evidence of a new reversible transition that takes place in Sn/Si(111):B. The system changes from an insulating $(2\sqrt{3}\times2\sqrt{3})R30°$ structure at room temperature to a $(\sqrt{3}\times\sqrt{3})R30°$ symmetry above 520 K ($2\sqrt{3}$ and $\sqrt{3}$ in the following). We explain this transition using a microscopic diffusive mechanism [26], where a Sn tetramer diffuses on the surface among 24 inequivalent ground states, giving rise to the $\sqrt{3}$ symmetry. This transition is reminiscent of other dynamical fluctuations transitions, but it includes as an essential novel ingredient the diffusion of Sn tetramers along the surface settling an order-disorder transition for the system.

STM experiments were performed in the experimental described in Ref. [29]. Photoemission experiments were performed at the CASSIOPEE beam line of SOLEIL synchrotron. A highly B-doped silicon substrate (10^{-3} Ω cm) was flashed up to 1500 K and annealed several hours at 1100 K. In the calculations, we have used a combination of different density functional theory (DFT) techniques i) local-orbital MD [30], to search for Sn/Si(111):B-$2\sqrt{3}$ atomic structures and to analyze the dynamics at different temperatures; ii) plane wave DFT [31], for a final refinement of the structures and for the calculation of the electronic structure; iii) a combination of a Keldysh Green's function formalism and DFT, to simulate the STM images, e.g., see [32].

Figure 1(a) shows the STM image for the new $2\sqrt{3}$ reconstruction induced by adsorption of Sn on a Si(111):B-$\sqrt{3}$ surface. After Sn deposition at high

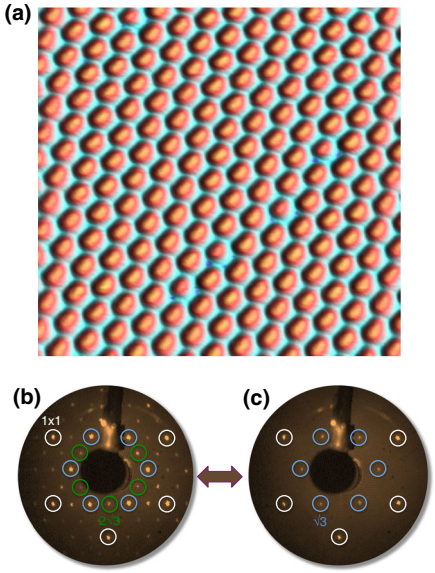

FIG. 1 (color online). (a) 15×14.5 nm^2 STM image of the Sn/Si(111):B-$2\sqrt{3}$ surface (−1.5 V, 0.02 nA). LEED patterns of (b) the $2\sqrt{3}$ phase ground state at room temperature and (c) the $\sqrt{3}$ phase above 520 K (70 eV beam energy). See Supplemental Material [33] for a video of the reversibility.

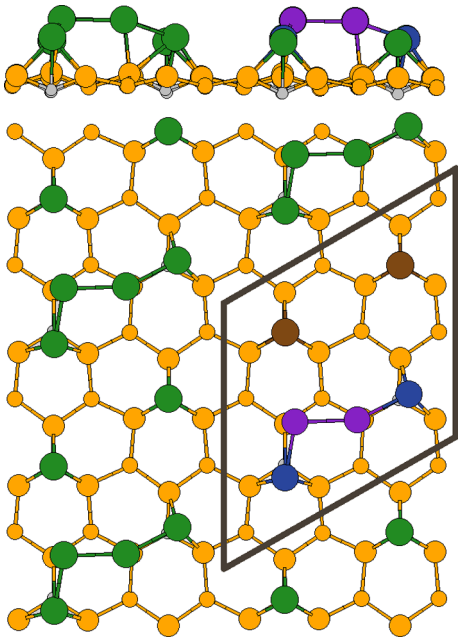

FIG. 2 (color online). Side and top views for the Sn/Si(111):B-$2\sqrt{3}$ atomic structure. Large, medium, and small balls correspond to Sn (green) and Si (orange) first and second layer atoms, respectively; small grey balls in the side view represent B atoms. Inside the unit cell (indicated by black solid lines) Sn adatoms, lateral, and central tetramer atoms are plotted in different colors (brown, blue, and purple, respectively).

temperature (900 K), the single circular spot in the $\sqrt{3}$ unit cell is replaced by an elongated bright spot per $2\sqrt{3}$ unit cell, with an apparent size of 8.5×6 Å^2, which can thus contain more than one atom. When the Sn/Si(111):B-$2\sqrt{3}$ is annealed above 520 K, the surface symmetry changes to a $\sqrt{3}$ in a fully reversible way, as observed by LEED [Figs. 1(b) and 1(c)]. In order to determine the Sn coverage and the number of equivalent Sn environments, we have performed core level spectroscopy (see [33]). The $2\sqrt{3}$ reconstruction corresponds to the surface saturation (i.e., 1/2 ML or six Sn atoms per unit cell) where the Sn atoms are in a similar charge state. In our modelization, we have thus considered more than 20 atomic structures with six Sn-atoms per $2\sqrt{3}$ unit cell and have analyzed for each (a) their relative stability, (b) their STM-image, (c) their electronic band structure, and (d) their possible phase transition from $2\sqrt{3}$ to $\sqrt{3}$, as a function of temperature. In our calculations, we have dynamically relaxed different initial configurations for the Sn atoms on the surface, including the replacement of the Si adatoms by Sn. The stability of surface reconstructions with different number of Si atoms, N_{Si}, is analyzed by DFT calculations for the surface energy $F = E_{\mathrm{TOT}} - \mu_{Si} N_{Si}$, where E_{TOT} is the total energy and μ_{Si} the Si chemical potential, which is equal to the total energy (per atom) of bulk Si [32,38].

Our analysis has led us to conclude that the $2\sqrt{3}$ structure is the one shown in Fig. 2, with four Sn atoms replacing the Si adatoms, plus a Sn dimer bonded to two of these Sn adatoms, forming a Sn tetramer; this structure is 0.2 eV lower than the next lowest energy structure that we have found. Figure 2 shows schematically how the Sn atoms saturate the dangling bonds (DB) of the Si surface. The isolated Sn adatoms are bonded to three Si atoms of the surface, passivating their DBs. In the tetramer, each lateral Sn atom is bonded to two Si DBs, while each central atom is placed above one of the remaining Si DB sites. Thus, each Sn atom is bonded to three atoms, while two electrons form a π bond associated with the tetramer Sn atoms. This geometry is highly degenerate, with 24 equivalent dispositions of the Sn tetramer and the two isolated Sn adatoms in the unit cell. As we will see, the interaction of Sn atoms with Si DB sites determines the atomic motion at high temperature, as Sn atoms dance on the surface between Si DB sites in a concerted fashion exploring the different ground states.

In Fig. 3, experimental and theoretical STM images are compared at different voltages. The agreement is excellent, the theoretical images showing even small asymmetries observed at high bias voltages, originated by the snakelike shape of the tetramer. The bright protusions shown by each tetramer are mainly associated with the two central Sn atoms of the tetramer that are ~0.9–1.0 Å higher than the other Sn atoms. This explains the similarity of our images with those obtained for the Sn/Si(111)-$2\sqrt{3}$ surface, that presents a Sn double layer and a melting transition [39,40]. We can discard a Sn double layer for our system by measuring the step height between Sn/Si(111):B-$2\sqrt{3}$ and

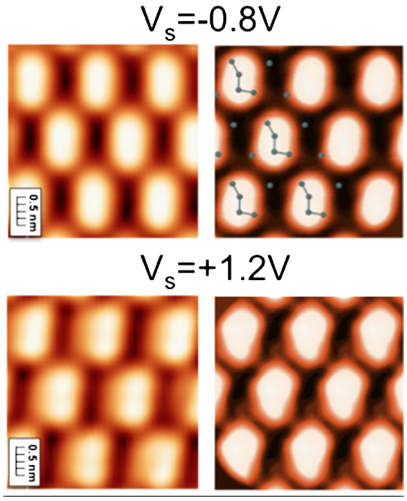

FIG. 3 (color online). Experimental STM images for the $2\sqrt{3}$ reconstruction (left panels) and theoretical STM images for the structural model of Fig. 2 (right panels). The top right figure shows Sn atomic positions.

Si(111):B-$\sqrt{3}$ domains. This height difference is only ~0.6 Å, clearly incompatible with a double layer model.

On the other hand, our model reproduces also the experimental band structure, Fig. 4(a). In the Sn-reconstructed surface, we find a low-dispersing feature around 300 meV of binding energy ($S1$) and a half-width of 100 meV; a weaker structure is also seen around 900 meV of binding energy ($S2$). The $S1$ surface feature does not reach the Fermi level, so the Sn/Si(111):B-$2\sqrt{3}$ is insulating at room temperature with low dispersing surface bands. The calculated band structure, shown in Fig. 4(b), has two very narrow surface bands around 300 meV ($S1'$) and 400 meV ($S1''$) of binding energy, in good agreement with the surface feature at 300 meV (S_1); the energy gap between $S1'$ and the first unoccupied surface band (not shown in the figure) is 400 meV, as corresponds to the semiconductor character of this surface. Figure 4(b) also shows two other surface bands located around 750 meV ($S2'$) and 900 meV ($S2''$) of binding energy in good agreement with the $S2$ feature of Fig. 4(a).

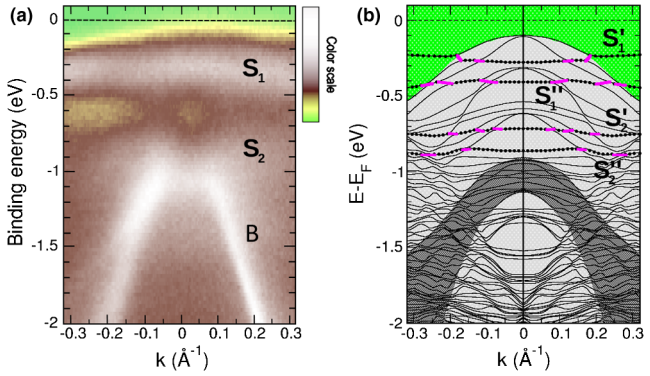

FIG. 4 (color online). Band structure for the RT-$2\sqrt{3}$ phase along $\bar{\Gamma}\bar{K}_{\sqrt{3}}$. (a) Experimental band structure at $h\nu = 27$ eV. S_1 and S_2 are Sn surface features and B is a bulk band. (b) Calculated band structure for the model in Fig. 2 showing the four surface states S_1', S_1'', S_2', and S_2'' associated with the Sn atoms. Pink lines are a guide to the eye.

The key question is how this model can explain the reversible phase transition as a function of temperature. In the reversible transitions mentioned above, the different ground state geometries correspond to *soft* distortions from an ideal geometry [17,19,41]. In the present case, however, Sn atoms have to break covalent bonds and jump between different Si DB sites to visit different ground states. Since local probes lack of subpicosecond resolution, we have analyzed the $2\sqrt{3} \leftrightarrow \sqrt{3}$ transition performing long (200–500 ps) DFT MD simulations at different temperatures. In all these motions, there are always four Sn atoms (per $2\sqrt{3}$ unit cell) oscillating around the positions of the adatoms of the initial Si(111):B-$\sqrt{3}$ substrate, defining a $\sqrt{3}$ symmetry. At low T (e.g., 300 K), Sn atoms oscillate around their equilibrium positions, preserving the $2\sqrt{3}$ symmetry. At high T (700 K), however, we find that the Sn atoms occasionally jump between different Si-DB sites, the tetramer thus moving along the surface visiting the different ground states of the system. As an example, Fig. 5 (left) shows one of these jumps, in which one Sn atom (orange line) moves to a nearby Si-DB position; after this jump, the system is in a different ground state, as indicated by the green lines. In this transition, the bond between the blue and orange Sn atoms is broken; at the same time, a new bond is formed (orange and grey Sn atoms). Figure 5 (right) shows a more complex transition between ground state configurations in which a central and lateral tetramer Sn atoms are both jumping and interchanging positions within

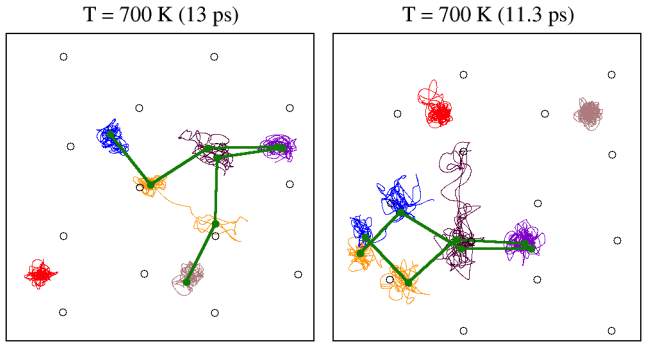

FIG. 5 (color online). Top view of the motion of the six Sn atoms (different colors) from DFT MD simulations at 700 K. The open circles indicate the (ideal) positions of the Si surface atoms (Si DB sites). The solid green lines indicate the initial and final configurations for the Sn tetramers. The left panel shows one temporal evolution during 13 ps, showing how the system jumps to a new ground state geometry. The right panel shows another temporal evolution of 11.3 ps showing a more complicated evolution of the concerted motion of the Sn adatoms. See the corresponding videos in the Supplemental Material [33].

the tetramer (see the videos for these and other transitions in the Supplemental Material [33]).

In summary, we have presented experimental and theoretical evidence for a reversible $\sqrt{3} \leftrightarrow 2\sqrt{3}$ transition for Sn/Si(111):B. The ground state structure contains a Sn tetramer and two Sn adatoms (per $2\sqrt{3}$ unit cell), and there are 24 degenerate ground state geometries. Above 520 K, the interface loses the $2\sqrt{3}$ symmetry in an apparent melting of the interface. This transition is explained by a novel mechanism in which the Sn atoms jump between different Si DB sites and the Sn tetramer diffuses along the surface, visiting in this way the different ground state geometries and giving rise to the observed $\sqrt{3}$ symmetry. This study opens perspectives in catalytic processes as Sn is a catalytic metal widely used for growing silicon or germanium nanowires in solar cells. We observe that Sn clusters wiggle on the surface without coalescing in bigger clusters that would reduce the active region for a catalysis reaction. Moreover, the movement of Sn clusters increases the cross section for capturing reactants. Finally, our results are the proof of concept that the amount of expensive catalytic (metallic) material could be reduced on less expensive Si substrates when operating at high temperatures, as in common catalytic reactions.

This work was supported by the French Agence Nationale de la Recherche (ANR) under Contract SurMott, No. NT-09-618999, and by Spanish Ministerio de Economía y Competitividad, Project No. MAT2014-59966-R.

W. S. and D. G. T. contributed equally to this work.

*Corresponding author.
antonio.tejeda@u-psud.fr

[1] B. N. J. Persson, Surf. Sci. Rep. **15**, 1 (1992).
[2] A. Tejeda, Y. Fagot-Revurat, R. Cortés, D. Malterre, E. G. Michel, and A. Mascaraque, Phys. Status Solidi (a) **209**, 614 (2012).
[3] P. Snijders and H. Weitering, Rev. Mod. Phys. **82**, 307 (2010).
[4] S. Qin, J. Kim, Q. Niu, and C. Shih, Science **324**, 1314 (2009).
[5] T. Zhang, P. Cheng, W.-J. Li, Y.-J. Sun, G. Wang, X.-G. Zhu, K. He, L. Wang, X. Ma, X. Chen, Y. Wang, Y. Liu, H.-Q. Lin, J.-F. Jia, and Q.-K. Xue, Nat. Phys. **6**, 104 (2010).
[6] G. Li, P. Höpfner, J. Schäfer, C. Blumenstein, S. Meyer, A. Bostwick, E. Rotenberg, R. Claessen, and W. Hanke, Nat. Commun. **4**, 1620 (2013).
[7] S. C. Erwin and F. J. Himpsel, Nat. Commun. **1**, 58 (2010).
[8] V. Y. Aristov, L. Douillard, O. Fauchoux, and P. Soukiassian, Phys. Rev. Lett. **79**, 3700 (1997).
[9] T. Tabata, T. Aruga, and Y. Murata, Surf. Sci. **179**, L63 (1987).
[10] L. Chaput, C. Tournier-Colletta, L. Cardenas, A. Tejeda, B. Kierren, D. Malterre, Y. Fagot-Revurat, P. Le Fèvre, F. Bertran, A. Taleb-Ibrahimi, D. G. Trabada, J. Ortega, and F. Flores, Phys. Rev. Lett. **107**, 187603 (2011).
[11] R. Cortés, A. Tejeda, J. Lobo, C. Didiot, B. Kierren, D. Malterre, E. G. Michel, and A. Mascaraque, Phys. Rev. Lett. **96**, 126103 (2006).
[12] S. Modesti, L. Petaccia, G. Ceballos, I. Vobornik, G. Panaccione, G. Rossi, L. Ottaviano, R. Larciprete, S. Lizzit, and A. Goldoni, Phys. Rev. Lett. **98**, 126401 (2007).
[13] G. Profeta and E. Tosatti, Phys. Rev. Lett. **98**, 086401 (2007).
[14] V. Derycke, P. Soukiassian, F. Amy, Y. Chabal, M. D'Angelo, H. Enriquez, and M. Silly, Nat. Mater. **2**, 253 (2003).
[15] F. Schmitt, P. S. Kirchmann, U. Bovensiepen, R. G. Moore, L. Rettig, M. Krenz, J. H. Chu, N. Ru, L. Perfetti, D. H. Lu, M. Wolf, I. R. Fisher, and Z. X. Shen, Science **321**, 1649 (2008).
[16] P. Hansmann, T. Ayral, L. Vaugier, P. Werner, and S. Biermann, Phys. Rev. Lett. **110**, 166401 (2013).
[17] D. G. Trabada and J. Ortega, J. Phys. Condens. Matter **21**, 182003 (2009).
[18] H. W. Yeom, S. Takeda, E. Rotenberg, I. Matsuda, K. Horikoshi, J. Schaefer, C. M. Lee, S. D. Kevan, T. Ohta, T. Nagao, and S. Hasegawa, Phys. Rev. Lett. **82**, 4898 (1999).
[19] C. Gonzalez, F. Flores, and J. Ortega, Phys. Rev. Lett. **96**, 136101 (2006).
[20] S. Wippermann and W. G. Schmidt, Phys. Rev. Lett. **105**, 126102 (2010).
[21] J. M. Carpinelli, H. H. Weitering, E. W. Plummer, and R. Stumpf, Nature (London) **381**, 398 (1996).
[22] J. M. Carpinelli, H. H. Weitering, M. Bartkowiak, R. Stumpf, and E. W. Plummer, Phys. Rev. Lett. **79**, 2859 (1997).
[23] J. Avila, A. Mascaraque, E. G. Michel, M. C. Asensio, G. LeLay, J. Ortega, R. Pérez, and F. Flores, Phys. Rev. Lett. **82**, 442 (1999).
[24] R. Cortés, A. Tejeda, J. Lobo-Checa, C. Didiot, B. Kierren, D. Malterre, J. Merino, F. Flores, E. G. Michel, and A. Mascaraque, Phys. Rev. B **88**, 125113 (2013).
[25] S. C. Erwin, Nature (London) **441**, 295 (2006).
[26] For diffusion of adatoms on metal MLs on Si(111) surfaces, see Refs. [27,28].
[27] S. C Jung and M. H. Kang, Phys. Rev. B **84**, 155422 (2011).
[28] S. Jeong and H. Jeong, Phys. Rev. B **81**, 195429 (2010).
[29] C. Didiot, A. Tejeda, Y. Fagot-Revurat, V. Repain, B. Kierren, S. Rousset, and D. Malterre, Phys. Rev. B **76**, 081404(R) (2007).
[30] J. P. Lewis, P. Jelínek, J. Ortega, A. A. Demkov, D. G. Trabada, B. Haycock, H. Wang, G. Adams, J. K. Tomfohr, E. Abad, H. Wang, and D. A. Drabold, Phys. Status Solidi (b) **248**, 1989 (2011).
[31] S. Baroni, A. Corso, S. de Gironcoli, and P. Giannozzi, Quantum EXPRESSO, 2005.
[32] C. González, P. C. Snijders, J. Ortega, R. Pérez, F. Flores, S. Rogge, and H. H. Weitering, Phys. Rev. Lett. **93**, 126106 (2004).
[33] See Supplemental Material at http://link.aps.org/supplemental/10.1103/PhysRevLett.114.196101 for the reversibility demonstration and modelisation, more information on the

electronic properties and simulation of STM images and the experimental coverage determination, which includes Refs. [34–37].

[34] H. Q. Shi, M. W. Radny, and P. V. Smith, Phys. Rev. B **66**, 085329 (2002).

[35] C. Tournier-Colletta, Ph.D. thesis, Université Henri Poincaré, 2011.

[36] J. M. Blanco, C. González, P. Jelínek, J. Ortega, F. Flores, and R. Pérez, Phys. Rev. B **70**, 085405 (2004).

[37] J. I. Martínez, E. Abad, C. González, F. Flores, and J. Ortega, Phys. Rev. Lett. **108**, 246102 (2012).

[38] J. E. Northrup, Phys. Rev. B **44**, 1419 (1991).

[39] T. Ichikawa and K. Cho, Jpn. J. Appl. Phys. **42**, 5239 (2003).

[40] P. E. J. Eriksson, J. R. Osiecki, K. Sakamoto, and R. I. G. Uhrberg, Phys. Rev. B **81**, 235410 (2010).

[41] R. Pérez, J. Ortega, and F. Flores, Phys. Rev. Lett. **86**, 4891 (2001).